

Atomic and Electronic Structure Evolution of ZIF-L Metal Organic Framework During Amorphization

Supriya Ghosh¹, Prashant Kumar² and K. Andre Mkhoyan¹

¹University of Minnesota, Twin Cities, Minneapolis, Minnesota, United States, ²University of Michigan, Ann Arbor, Ann Arbor, Michigan, United States

Zeolitic imidazolate frameworks (ZIFs) are metal organic frameworks (MOFs) having tetrahedral coordination of 2-methylimidazole linkers to the Zn metal centers, forming a porous framework identical to zeolites [1]. Amorphization of crystalline MOFs can be carried out by electron-beam or X-ray irradiation, both of which have been used for patterning amorphous MOFs at sub-micron-scales [2, 3]. In this study, we use electron diffraction and EELS at very low dose rates simultaneously to monitor the amorphization of the crystalline framework and changes in the organic linker molecules. The changes in chemical bonds of C and N atoms that are part of the linker molecules are evaluated by measuring changes in core-level EELS fine structures of C and N K-edges.

ZIF-L MOFs used here were synthesized in water using $\text{ZnNO}_3 \cdot 6\text{H}_2\text{O}$ as the source of the metal and 2-methylimidazole as the organic linker based on a process described in Chen et. al. [4] and, was purified by washing in DI water 3 times. The resulting particles with a leaf-like morphology are shown in Figure 1(a). Dose-dependent electron diffraction patterns were recorded at multiple dose-rates to evaluate the beam-induced damage of these ZIF-L MOF samples [5]. Similarly, dose-dependent EELS data were acquired to evaluate the effects of beam damage on the atomic bonds of C and N in the linkers. The experiments were carried out using FEI Technai G² F30 (S)TEM and an aberration-corrected FEI Titan 60-300 (S)TEM, which is equipped with a CEOS DCOR probe corrector, monochromator, and Gatan Enfinitum ER EELS spectrometer. All EELS data were acquired at very low probe currents.

First, selected area electron diffraction patterns obtained (Figure 1(b)) were used to evaluate the degree of damage (critical dose 75-100 $\text{e}/\text{\AA}^2$). The radially averaged diffraction intensities are separated into crystalline and amorphous components, as shown in Figure 1(c). Then changes of the fraction of each component was evaluated with dose accumulation (Figure 1(d)). Further, changes in the bonding of the linker molecules were studied by tracking changes in the core level EELS fine-edge structures of the C and N K-edges (π^* and σ^* peaks). The splitting of the σ^* peak at 297 eV in C K-edge disappears above an accumulated dose of 75 $\text{e}/\text{\AA}^2$, suggesting C-C / C-N bonds in the linker breaking (Figure 2(a)). Furthermore, changes in low-loss region of EELS were also measured as a function of dose accumulation, since it contains two different plasmon excitations corresponding to π^* and σ^* bonds (Figure 2(b)). The decay of these peaks suggests a possible collapse of ZIF-L pores with additional changes in the linker molecules [7].

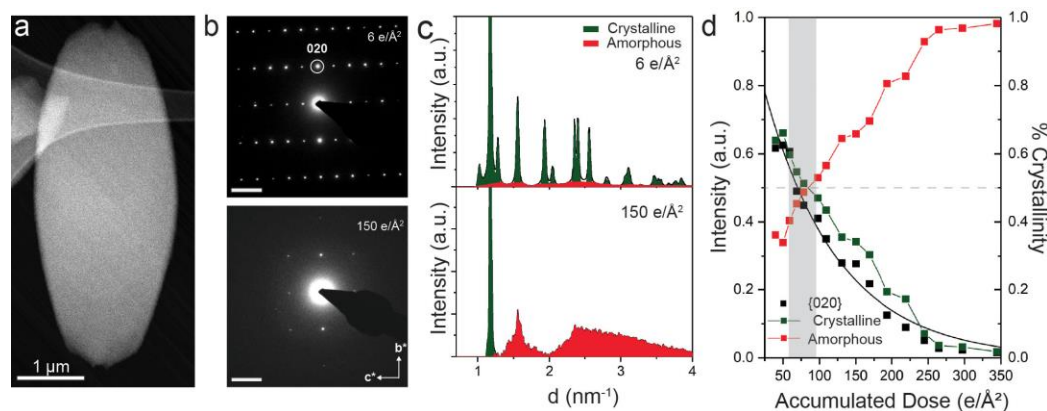


Figure 1. (a) HAADF-STEM image of a ZIF-L particle showing the leaf-like morphology. (b) Electron diffraction patterns from a ZIF-L particle at two accumulated doses. Scale bar is 1 nm^{-1} . (c) Radially averaged, background-subtracted intensities of the electron diffraction pattern shown in (b) highlighting the crystalline and amorphous contributions to the total diffraction intensity. (d) The integrated intensity of the [020] diffraction spot as a function of accumulated dose showing exponential decay along with the fraction of amorphous and crystalline contents based on diffraction intensities.

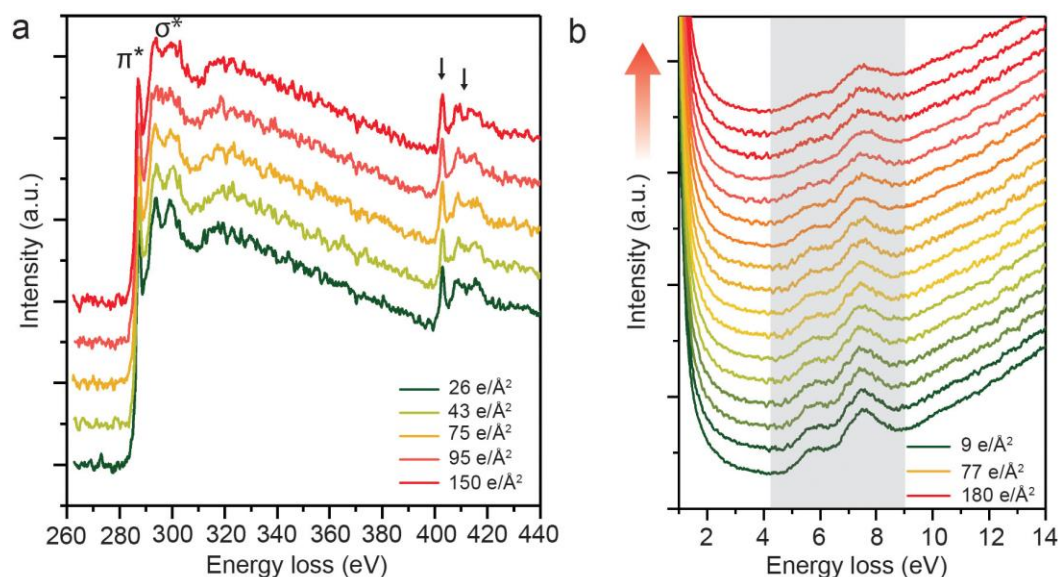


Figure 2. A set of EELS Spectra from ZIF-L obtained as a function of accumulated dose. (a) Core-loss EELS spectra of C and N K-edges as a function of accumulated dose showing changes in the fine structure of the C and N K-edges (π^* and σ^* peaks). (b) Low-loss spectra showing the decay of two peaks at 5.85 eV and 7.5 eV with dose accumulation acquired in steps of 10 – 15 $\text{e}/\text{\AA}^2$.

References

- [1] Park K. S. et al., PNAS Jul 2006, **103** (27) 10186-10191.
- [2] Conrad S. et al., Angew.Chem.Int.Ed.**2018**, 57, 13592–13597.
- [3] Widmer R. N. et al.; Phys. Chem. Chem. Phys., 2019, 21, 12389.
- [4] Chen R., et al., Chem. Commun., 2013, **49**, 9500.
- [5] D. Zhang et al., Science **359** (2018), 675-679.
- [6] Guo C. et al., Adv. Funct. Mater. **2015**, 25, 6071-6076.
- [7] This work was supported by the NSF MRSEC under award number DMR-1420013.